ISSN 2075-3810 (Print), ISSN 2075-3829 (Online)

БІОФІЗИЧНИЙ ВІСНИК, 2025, Вип. 54 BIOPHYSICAL BULLETIN, 2025, Iss. 54

MOLECULAR BIOPHYSICS

Original article

https://doi.org/10.26565/2075-3810-2025-54-01

UDC 577.322:004.94:578.834.1

IN SILICO ANALYSIS OF BINDING SITES FOR POTENTIAL INHIBITORS TARGETING THE COMPLEX OF FURIN PROTEASE AND THE SARS-COV-2 SPIKE PROTEIN

N. V. Khmil[1,2*], A. V. Shestopalova[2], V. G. Kolesnikov[2]

[1]Kharkiv National University of Radio Electronics, 14 Nauky Ave., Kharkiv, 61166, Ukraine;
[2]O. Ya. Usikov Institute for Radiophysics and Electronics National Academy of Sciences of Ukraine, 12 Acad. Proskura str., Kharkiv, 61085, Ukraine
**Corresponding author: khmilnatali@gmail.com*
Submitted April 28, 2025; Revised July 7, 2025;
Accepted August 29, 2025

Background: COVID-19 is an infectious disease caused by severe acute respiratory syndrome coronavirus 2 (SARS-CoV-2). Efforts to fight the virus include the development and investigation of vaccines, monoclonal antibodies, and specific antiviral drugs targeting key stages in the viral life cycle.
Objectives: The aim of this study is to investigate the potential sites of furin protease binding to the S protein in different conformations and to evaluate the binding affinity of non-specific antiviral drugs and the macrocyclic peptidomimetic inhibitor 8 (PI8) to the S protein–furin protease complex using a molecular docking approach.
Material and Methods: The three-dimensional structures of the S protein (PDB IDs: 6VYB, 6VXX, 7VHJ) from the Protein Data Bank (www.rcsb.org) were docked with furin protease (PDB ID: 5JXG) using the ClusPro 2.0 server. Non-specific antiviral drugs, such as remdesivir, chloroquine, favipiravir, nelfinavir, and PI8, were docked onto 6VYB-5JXG, 6VXX-5JXG, and 7VHJ-5JXG complexes using the AutoDock Vina program. The ligands were energy-minimized using the Universal Force Field (UFF) and converted to PDBQT format with OpenBabel. Protein optimization was performed using AutoDock Tools. Docking results were visualized using the Discovery Studio 2024 Visualizer.
Results: The binding affinity of the studied ligands with the S protein-furin protease complexes was verified by molecular docking studies. PI8, nelfinavir, and remdesivir showed high binding affinity with the 7VHJ-5JXG structure due to the fully modeled structure of the furin cleavage site. The best docking scores of PI8 with 6VYB-5JXG, 6VXX-5JXG, and 7VHJ-5JXG complexes were -9.7 kcal/mol, -9.5 kcal/mol, and -9.9 kcal/mol, respectively. The interaction between the S protein-furin complexes and PI8 involves specific amino acid residues, primarily within the catalytic site of furin and the reactive site loop of PI8. Docking studies showed that remdesivir acts directly on the furin cleavage site of the S protein (in the 7VHJ-5JXG complex), forming energetically favorable interactions through hydrogen bonds and hydrophobic contacts, with a high binding affinity (binding energy score is -9.1 kcal/mol). The energetically favorable interactions of the 6VYB-5JXG, 6VXX-5JXG, and 7VHJ-5JXG complexes with nelfinavir are also confirmed by low binding energy scores of -8.2 kcal/mol, -8.9 kcal/mol, and -9.3 kcal/mol, respectively.
Conclusion: According to the results of molecular docking, PI8, nelfinavir, and remdesivir demonstrate energetically favorable interactions with the studied complexes and can be considered promising inhibitors targeting the SARS-CoV-2 S protein–furin protease complexes.
KEY WORDS: SARS-CoV-2 spike protein; furin protease; antiviral drugs; molecular docking; human health.

Citation: Khmil NV, Shestopalova AV, Kolesnikov VG. *In silico* analysis of binding sites for potential inhibitors targeting the complex of furin protease. Biophysical Bulletin. 2025;54:9–26. https://doi.org/10.26565/2075-3810-2025-54-01

COVID-19 is an infectious disease caused by the severe acute respiratory syndrome coronavirus 2 (SARS-CoV-2), which has affected more than 7.0 million people worldwide [1]. Over the past five years, the virus has spread rapidly across countries due to its ability to transmit through respiratory pathways. Additionally, the virus has the capacity for asymptomatic and pre-symptomatic transmission. Therefore, individuals infected with SARS-CoV-2 can transmit the virus before showing symptoms — such as respiratory distress, headache, fatigue, sore throat, and high fever — or even without developing symptoms, making detection and containment particularly challenging. The combination of immune evasion and high infectivity may also contribute to the widespread transmission of SARS-CoV-2 [2].

Efforts to fight the virus include the development of vaccines, monoclonal antibodies, and specific antiviral drugs targeting key stages in the viral life cycle, with research on these treatments currently ongoing [3, 4]. Most studies focus on the numerous structural and nonstructural viral proteins encoded by SARS-CoV-2, including the SARS-CoV-2 spike glycoprotein (S protein), papain-like protease (PLpro), and the main protease (Mpro) [5, 6]. Additionally, studying human cell proteases, such as furin and type II transmembrane serine protease (TMPRSS2), is crucial for understanding the mechanisms involved in the activation of the SARS-CoV-2 S protein.

The attachment of SARS-CoV-2 to the host cell is a critical step in the infection process, mediated by interactions between the S protein and the host cell's angiotensin-converting enzyme 2 (ACE2) receptor. The viral S protein is a structural trimeric protein, approximately 1,273 amino acids long, that belongs to the class I viral fusion proteins [7]. The S protein consists of the S1 subunit, which contains a signal peptide and a receptor-binding domain (RBD), and the S2 subunit, which includes the fusion peptide (FP), heptapeptide repeat sequences 1 and 2 (HR1, HR2), the transmembrane domain (TM), and the cytoplasmic domain [8]. The S1 and S2 subunits of the S protein are separated by a cleavage site recognized by furin-like proteases during its biogenesis in infected cells. Additionally, the S2 subunit contains an S2' cleavage site located immediately upstream of the first FP, exposing the FP, facilitating membrane fusion. The TM domain anchors the S protein to the viral envelope, while the HR1 and HR2 regions help form the post-fusion structure [9]. The dynamic transitions among the prefusion "open," postfusion "closed," and intermediate "semi-open" conformations are essential for the S protein's role in facilitating viral entry [10, 11]. The proteolytic activation of the S protein by host proteases is necessary to convert its precursor form into a biologically active form, enabling the subsequent fusion of viral and cellular membranes.

Upon binding with the ACE2 receptor, the S protein is processed by host cell proteases at two distinct sites. The furin protease cleaves the S1/S2 site, which contains multiple arginine residues [12]. Additionally, TMPRSS2 targets the S2′ site, priming the S protein and facilitating membrane fusion [13]. As a result of this priming, the N-terminal S1 domain binds to the host ACE2 receptor via the receptor-binding domain, while the C-terminal S2 domain undergoes significant structural transformations. These transitions from prefusion conformations to transient intermediates enable its insertion into the target host membrane [14].

The SARS-CoV-2 S protein has a cleavage site (682Arg-683Arg-684Ala-685Arg) at the S1/S2 boundary, which is cleaved by furin to prime the S protein for TMPRSS2 protease processing [15]. The furin cleavage site is unique to the SARS-CoV-2 S protein and is lacking in other coronaviruses, such as SARS-CoV, making it particularly efficient at utilizing host proteases for entry [16, 17]. This fusion event enables the viral genome to be released into the host cell cytoplasm, where it begins the replication process. Furin inhibition can block this important activation step, preventing the virus from effectively infecting host cells. Therefore, host molecules essential for the completion of viral replication and infection are emerging as potential targets for drug development [18].

Numerous well-known drugs with different pharmacological properties have been tested and used to treat various diseases, including COVID-19 [19–21]. The ligands selected for our study, such as remdesivir, nelfinavir, and favipiravir, have been investigated as potential candidates for inhibiting the spread of the coronavirus using *in silico*, *in vitro*, and *in vivo* methods within the framework of anti-COVID therapy protocols. Evidence suggests that these drugs can inhibit specific proteins, such as proteases and the S protein binding site on ACE2, which are critical for coronavirus infection, by forming stable complexes with them [22–24]. However, for some drugs, such as chloroquine and PI8, no reliable data confirms the presence of target molecules in SARS-CoV-2 [25].

Given that the virus is constantly evolving, it is crucial to continue searching for drugs capable of forming stable complexes with various critical protein systems of SARS-CoV-2. Due to the absence of a resolved structure for the region containing the furin cleavage site, it remains unclear whether furin can bind to additional sites on viral S glycoproteins to cleave them. Furthermore, understanding the effect of antiviral drugs on these complexes is essential. Therefore, elucidating the mode of interaction between furin and the spike glycoprotein will be critical for the effective design of antiviral drugs and antibodies.

The aim of this study is to investigate the potential sites of furin protease binding to the S protein in different conformations and to evaluate the binding affinity of non-specific antiviral drugs and the macrocyclic peptidomimetic inhibitor 8 (PI8) to the S protein–furin protease complex using a molecular docking approach.

MATERIALS AND METHODS

The three-dimensional structures of the S protein in its "open" (PDB ID: 6VYB), "closed" (PDB ID: 6VXX), and modified furin site (PDB ID: 7VHJ) conformations were obtained from the Protein Data Bank (www.rcsb.org). The 6VYB, 6VXX, and 7VHJ structures represent the best available experimental models of the S protein trimer in distinct conformational states, each of which is biologically relevant for spike activation and processing. In the study, these proteins were docked with furin protease (PDB ID: 5JXG) using the ClusPro 2.0 server. As the PDB files lacked hydrogen atoms, Kollman charges were assigned to match the electrostatic potentials, and hydrogen atoms were added using AutoDock Tools to optimize the proteins appropriately. The protonation states of amino acid residues at pH 7 were verified using PROPKA 3.1 [26]. In the next stage, non-specific antiviral drugs, including remdesivir, chloroquine, favipiravir, nelfinavir, and PI8, were docked onto the three constructed targets via the ClusPro 2.0 server — 6VYB-5JXG, 6VXX-5JXG, and 7VHJ-5JXG.

Ligands were downloaded in Structural Data File (SDF) format from the PubChem database (www.pubchem.ncbi.nlm.nih.gov). Log P values for all ligands were obtained from the PubChem database (https://pubchem.ncbi.nlm.nih.gov), where they were reported following calculation using the XLogP3 3.0 algorithm. XLogP3 employs an atom-additive (AA) method that estimates log P by summing the contributions of individual atoms based on their chemical environments. The structural formulas and some physicochemical properties of the studied ligands are shown in Figure 1.

Molecular docking was performed using the AutoDock Vina program [27]. Before docking, the ligands were minimized in energy using the Universal Force Field (UFF) and converted to PDBQT format with OpenBabel [28]. All docking studies were conducted as target docking, with the grid box encompassing the interacting chains of the S protein and furin protease. The grid box dimensions were set to 70 Å×70 Å×70 Å with a grid spacing of 0.508 Å. To increase the likelihood of identifying the global minimum of the scoring function, the exhaustiveness parameter in AutoDock Vina was set to 50. High-affinity binding complexes were subsequently analyzed using Discovery Studio 2024 Client software.

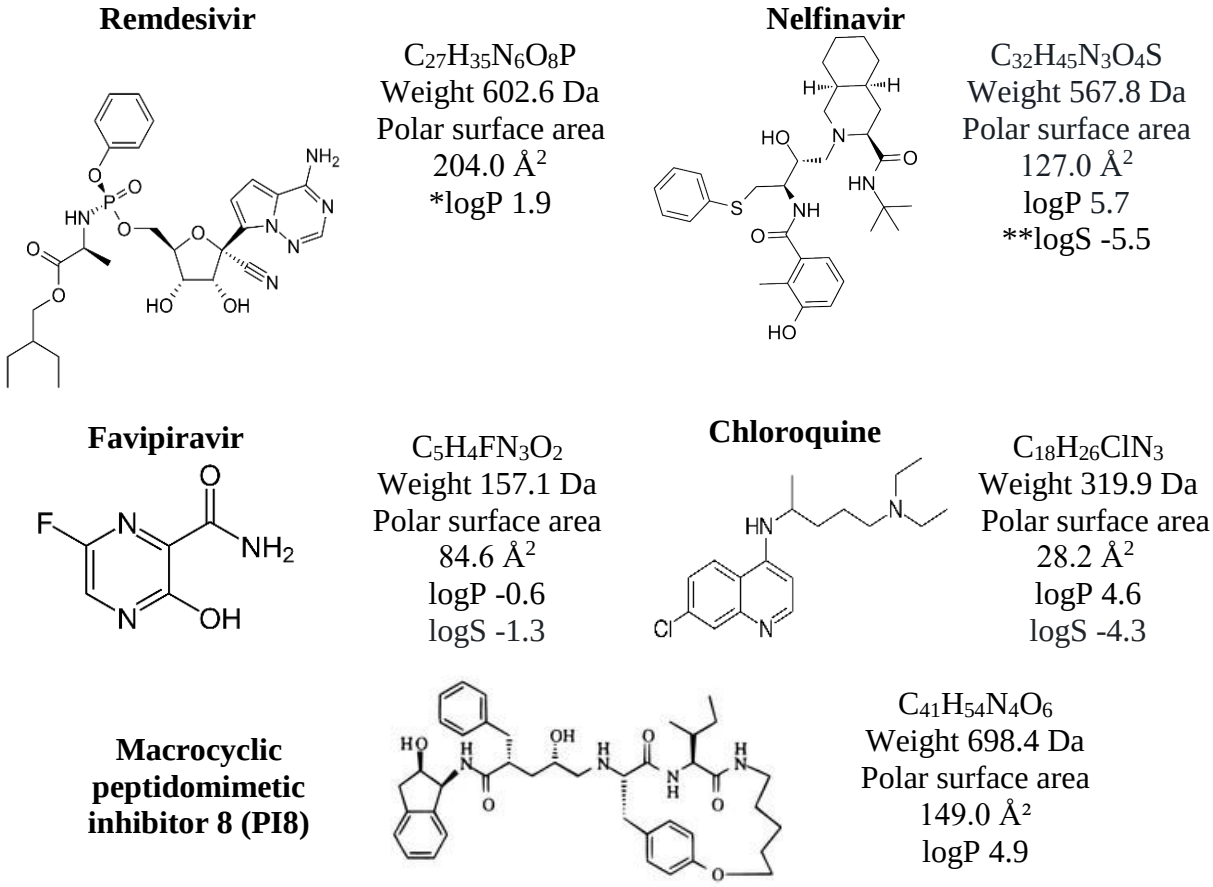

Fig. 1. Structures and physicochemical properties of ligands (www.pubchem.ncbi.nlm.nih.gov).
*logP — refers to the logarithm of the octanol/water partition coefficient as a measure of hydrophobicity of a compound;
**logS — directly related to the water solubility of a drug.

RESULTS AND DISCUSSION

The activation of the S glycoprotein by the host protease furin is an essential step in the replication of SARS-CoV-2. Furin protease represents a highly selective serine protease that binds with the S protein and activates it via proteolytic cleavage [29]. The inhibition of the S protein-furin protease complex is a promising approach for the treatment of COVID-19. Therefore, protein-protein complexes are important targets for the development of antiviral drugs, as the specificity of these interactions determines ligand binding affinity and the effectiveness of therapy.

The docking of the S protein in its "open," "closed," and modified furin site conformations with the furin protease was performed using the ClusPro 2.0 web-based server. This server utilizes a docking program based on the Fast Fourier Transform (FFT) correlation approach, employing pairwise potentials [30]. It selects the centers of highly populated clusters of low-energy structures rather than relying solely on the lowest-energy conformations.

The interaction energy between the two proteins is expressed as:

$$E = w_1 E_{rep} + w_2 E_{attr} + w_3 E_{elec} + w_4 E_{DARS},$$

where E_{rep} and E_{attr} — the repulsive and attractive forces described by the van der Waals interaction energy; E_{elec} is an electrostatic energy; E_{DARS} is a pairwise structure-based potential; w_1, w_2, w_3, and w_4 are the weight coefficients.

To analyze molecular interactions between the amino acid residues of protein structures, we used the generated models with a balanced parameter set. The weight coefficients used were:

w_1 = 0.4, w_2 = -0.4, w_3 = 600, and w_4 = 1.0. The protein-protein molecular docking studies revealed that the SARS-CoV-2 S protein in its different conformations binds to the furin protease, with binding energy scores presented in Table 1.

Table 1. Binding energy score of the SARS-CoV-2 S protein in different conformations with furin protease using Cluspro web server

Complex	Cluster	Representative	Binding energy score, kcal/mol
6VYB-5JXG	1	Center	-222.2
		Lowest energy	-254.7
6VXX-5JXG	1	Center	-220.9
		Lowest energy	-236.8
7VHJ-5JXG	1	Center	-213.7
		Lowest energy	-235.8

In Table 1, the center energy is the average interaction energy of the similar docking poses within a first cluster. The center energy is calculated for the pose that represents the center of the cluster (i.e., the most representative pose of that cluster). The lowest energy refers to the interaction energy of the pose with the lowest energy value within a first cluster. This represents the most energetically favorable pose among all poses in the cluster. The protein-protein docking of furin and the S protein in "open" conformation showed the binding affinity of furin with the lowest energy of -254.7 kcal/mol, which can be considered a potential candidate for further analysis, like the other two structures.

The unmodeled structure of the region containing the furin cleavage site of the S protein structures from the PDB in both the "open" (6VYB) and "closed" (6VXX) conformations has significantly influenced the outcomes of our modeling. Most researchers have reported some success in reconstructing the structure of the furin cleavage site of 6VYB structure after successfully modeling the entire SARS-CoV-2 S protein using the Protein Homology/Analogy Recognition Engine [31]. It was found that an antiparallel β-sheet connects the S1 and S2 regions of the S protein, comprising a few amino acid residues Arg-Arg-Ala-Arg in a short loop. Some acid residues protrude out of the main body of the SARS-CoV-2 S protein, which forms an antiparallel β-sheet along with a short loop comprising a furin cleavage site.

Our study demonstrates that furin can interact with the S protein outside the furin cleavage site, exhibiting high binding affinity (Table 1). This finding suggests alternative mechanisms for the S protein-furin interactions. In the 6VYB-5JXG and 6VXX-5JXG complexes, furin predominantly interacts with the receptor-binding domain of the S1 subunit, specifically with regions not designed for direct cleavage. Such interactions could arise from electrostatic or hydrophobic contacts between the proteins. In the 7VHJ-5JXG complex, the interacting amino acids are located near the fusion peptide (FP) and heptapeptide repeat sequence 1 (HR1), owing to the presence of the cleavage site. The results of N. Vankadari using molecular dynamics and computational model-based selective docking and simulation show that SARS-CoV-2 spike glycoprotein amino acid residues from Asp657 up to Gln690 are the prime residues interacting with the furin protease; this is mediated via van der Waals bonds and hydrogen bonding [32].

Alternative pathways for the S protein activation and hydrolysis are being investigated using molecular docking analysis and immunoblotting to identify precisely possible cleavage

sites to prevent viral entry into the target cell [33]. The identification of cathepsin cleavage sites in the S1/S2 fusion peptide region – not at the canonical site – suggests their assistance in activating cleavage of the S protein to promote membrane fusion [34]. Therefore, our results provide valuable insights into how furin interacts with additional regions of the S protein and affects its function.

AutoDock Vina program performs molecular docking and virtual screening of ligands with proteins, predicting noncovalent interactions and the binding affinity using a scoring function that is considered as the sum of intermolecular and intramolecular contributions. In this study, the binding energy scores of remdesivir, chloroquine, favipiravir, nelfinavir, and PI8 towards the S protein-furin protease complex were calculated by Autodock Vina 1.1.2 software. Autodock results demonstrated that these ligands can successfully dock with the SARS-CoV-2 S protein-furin complexes, as indicated by the AutoDock Vina scores presented in Table 2. The docked models with the lowest binding energy scores indicated the most energetically favorable interactions between the ligands and the target proteins.

Table 2. Binding energy score of studied ligands with target the SARS-CoV-2 S protein-furin protease complex

Ligand	Binding energy score, kcal/mol		
	6VYB-5JXG	6VXX-5JXG	7VHJ-5JXG
PI8	-9.7	-9.5	-9.9
Nelfinavir	-8.2	-8.9	-9.3
Remdesivir	-7.8	-8.2	-9.1
Chloroquine	-5.9	-6.3	-7.4
Favipiravir	-5.8	-5.9	-6.9

To verify the correctness of the above-described docking procedure, we have carried out re-docking calculations. The predictive power of docking in identifying binding sites of the studied ligands was assessed in PyMol by testing the SARS-CoV-2 spike protein (S protein) in different conformations from the PDB database with the studied ligands (PDB IDs: 7QG7, 3EL0, 7AAP, 4V2O, 1D4K). The RMSD between the ligand's original pose and the docking pose was less than 2 Å. So comparative analysis showed that AutoDock Vina demonstrated good agreement in re-docking these protein-ligand complexes.

According to Table 2, the highest binding affinity was observed for 7VHJ-5JXG docked by PI8, with an AutoDock Vina score of -9.9 kcal/mol. The amino acids involved were Arg214 from the C chain of the S protein and Asp258 from furin, interacting through electrostatic forces, such as π–cation and π–anion contacts. Additionally, Trp64 from the C chain of the S protein, along with Leu227 and His364 from furin, interacted via hydrophobic forces (π-sigma, π-alkyl). Furthermore, Asp191 of furin formed a hydrogen bond (Fig. 2).

The PI8 interacts with the 6VYB-5JXG with a binding energy score of -9.7 kcal/mol. In this case, the molecular binding is stabilized through hydrogen bonds with Ser253, His364 and Ser368 of furin, as well as hydrophobic interactions through five amino acid residues, including Arg193, His194, Leu227, Asn295, and Thr365 of furin. Additionally, a π–anion interaction with Asp258 is observed (Fig. 3).

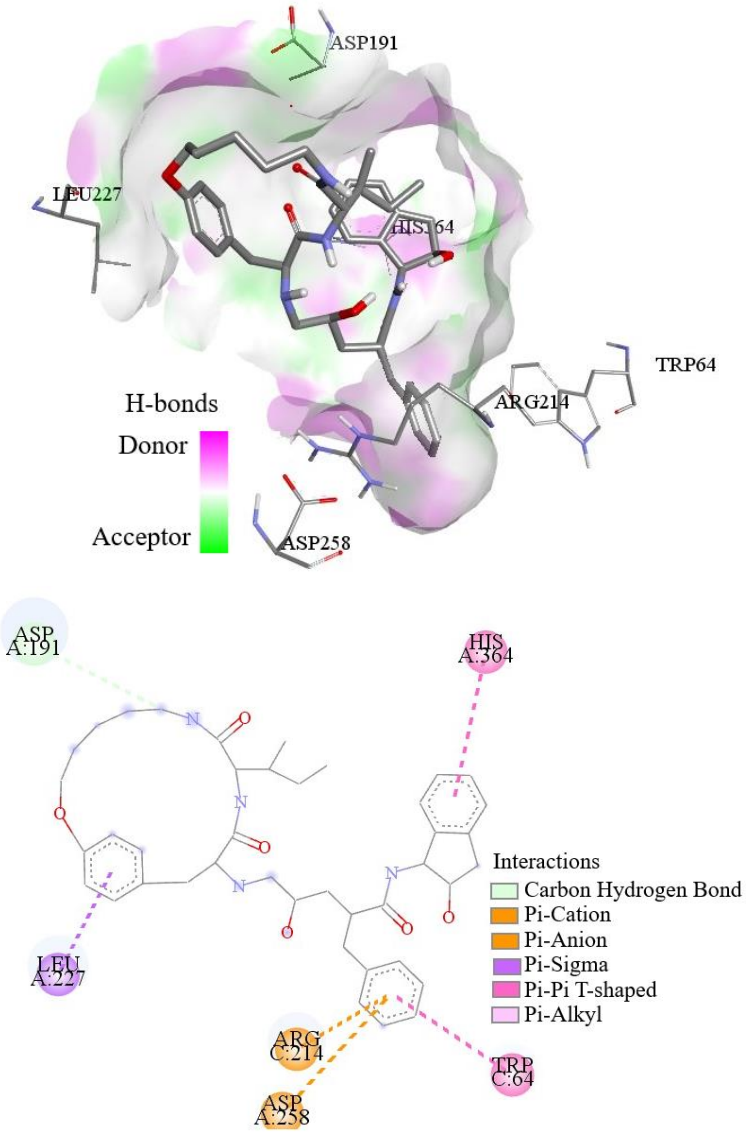

Fig. 2. The 3D and 2D representations of the complex 7VHJ-5JXG and its molecular interactions with PI8. Figures obtained with Discovery Studio software. The interacting residues of corresponding chains of the S protein and furin protease with PI8 (coloring by element, all C atoms of ligand are in dark gray, red — O, gray — H, blue — N) are labeled and shown as stick models. The ligand interaction diagram of PI8 with the 7VHJ-5JXG complex is shown, and the types of intermolecular interactions are labeled.

The PI8 also interacts with high binding affinity to 6VXX-5JXG, which is -9.5 kcal/mol. The molecular interaction is facilitated by hydrogen bonds with Tyr28 and Gly366 of furin, and hydrophobic interactions through residues Phe32, His194, Leu227, and Ser253 of furin. Additionally, a π–anion interaction occurs with Asp154 (Fig. 4).

It is also necessary to note that PI8 has a lipophilicity of logP = 4.9, which allows it to bind specifically and with high affinity to all the studied complexes, interacting with residues such as Leu227, Trp64, Ala292, Ser253, and Ser368, as illustrated in Figs. 2–4.

Our docking study suggests that PI8 could potentially act by inhibiting furin's interaction with the SARS-CoV-2 S glycoprotein at the binding sites, regardless of the conformation state of the S protein. The interaction between the S protein-furin complexes and PI8 involves specific amino acid residues, primarily within the active (catalytic) site of furin and the reactive site loop of PI8. As shown in the figures above, these interactions include hydrogen bonds, van

der Waals forces, and hydrophobic interactions. Our results are consistent with Van Lam's findings that the peptide-based drugs bind furin protease with higher affinity than other drugs [35].

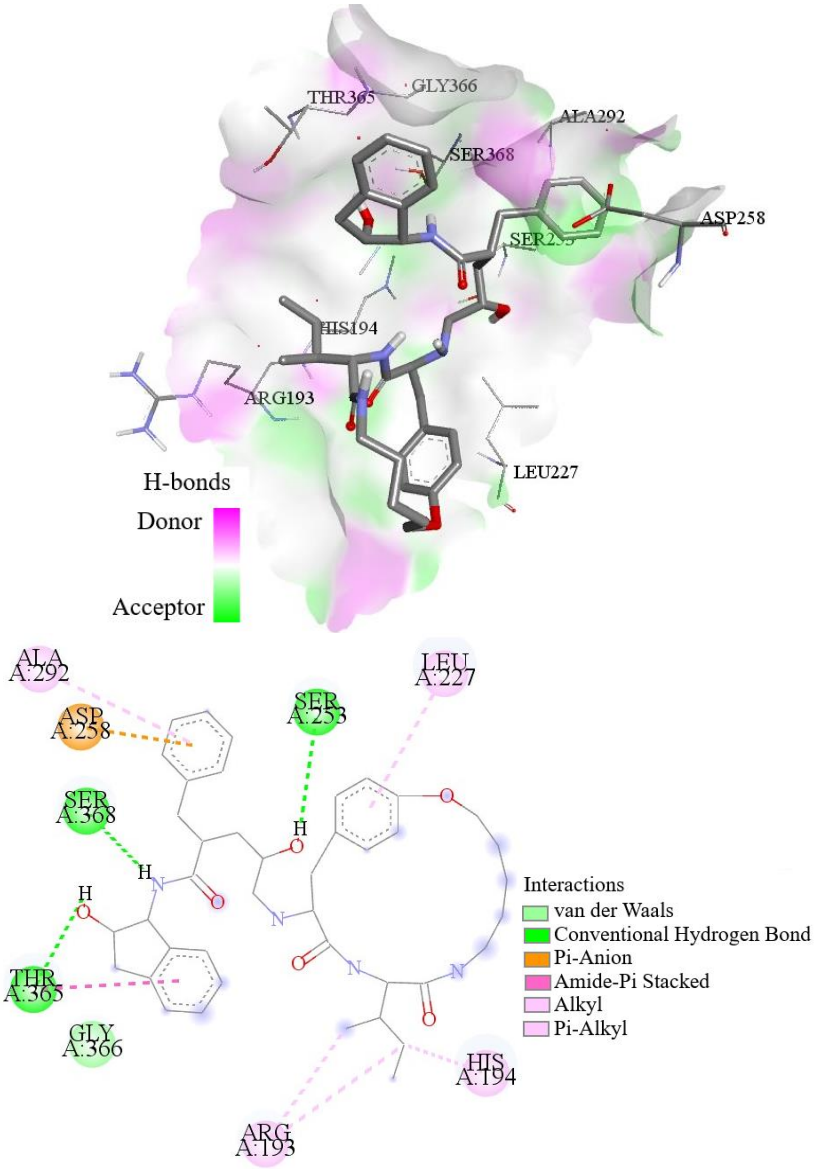

Fig. 3. The 3D and 2D representations of the complex 6VYB-5JXG and its molecular interactions with PI8. Figures obtained with Discovery Studio software. The interacting residues of furin protease with PI8 (coloring by element, all C atoms of ligand are in dark gray, red — O, gray — H, blue — N) are labeled and shown as stick models. The ligand interaction diagram of PI8 with the 6VYB-5JXG complex is shown, and the types of intermolecular interactions are labeled.

It is known that remdesivir inhibits the polymerase activity of the viral RNA-dependent RNA polymerase (RdRp) via RNA chain termination, thereby inhibiting SARS-CoV-2 replication and transcription [36]. Remdesivir also binds to Mpro, but with slightly weaker affinity than to RdRp [37]. As shown by Nguyen et al., the binding mechanisms of remdesivir to these two targets differ in that electrostatic interactions are the main force stabilizing the RdRp–remdesivir complex, while van der Waals interactions dominate in the Mpro–remdesivir case. Remdesivir demonstrated considerable binding affinity with the S protein in its "closed" conformation (6XXV) by forming hydrogen bonds with amino acid residues in the RBD and

HR1 sequence [38]. However, the binding affinity for the S protein in its "open" conformation was slightly lower, which is associated with the involvement of the transmembrane domain of the S protein. These results are consistent with our study, which found that the binding affinity of remdesivir to the 6VXX-5JXG complex was higher than that to the 6VYB-5JXG complex: -8.2 kcal/mol vs. -7.8 kcal/mol.

In the complex 6VYB-5JXG, remdesivir forms hydrophobic interactions only with the furin protease (Fig. 5).

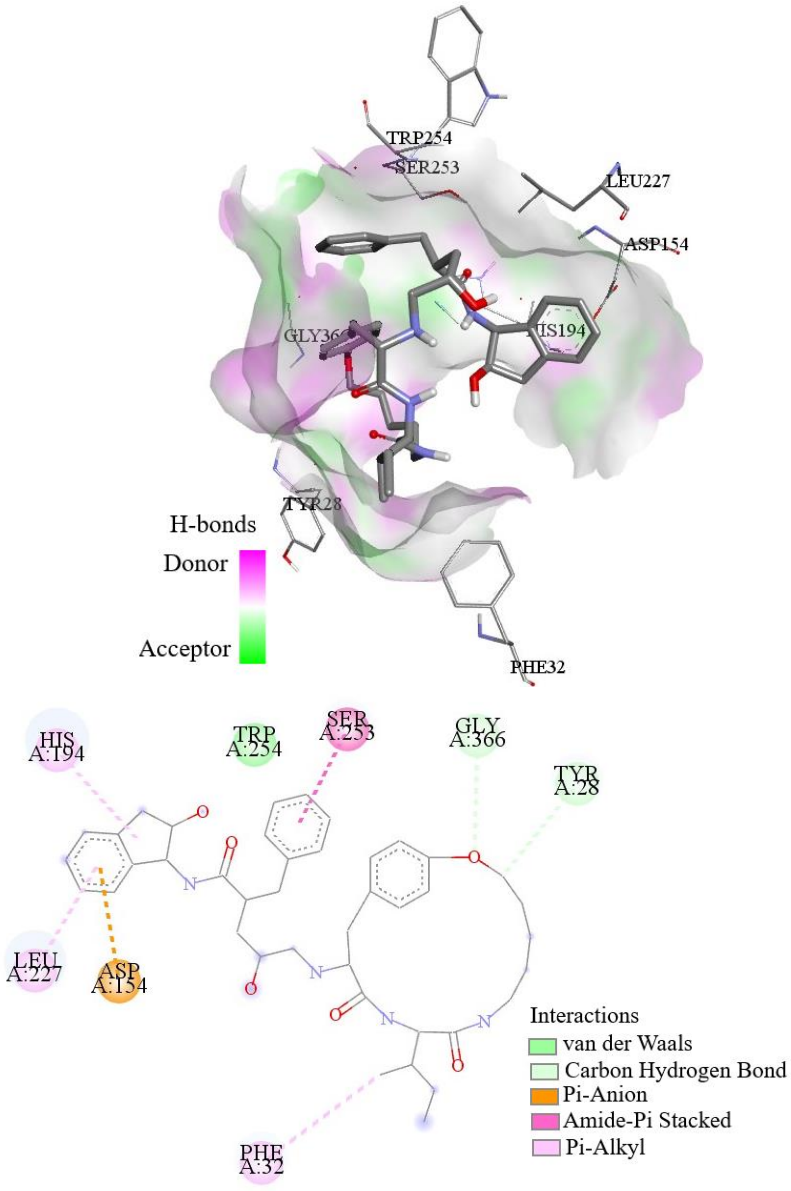

Fig. 4. The 3D and 2D representations of the complex 6VXX-5JXG and its molecular interactions with PI8. Figures obtained with Discovery Studio software. The interacting residues of furin protease with PI8 (coloring by element, all C atoms of ligand are in dark gray, red — O, gray — H, blue — N) are labeled and shown as stick models. The ligand interaction diagram of PI8 with the 6VXX-5JXG complex is shown, and the types of intermolecular interactions are labeled.

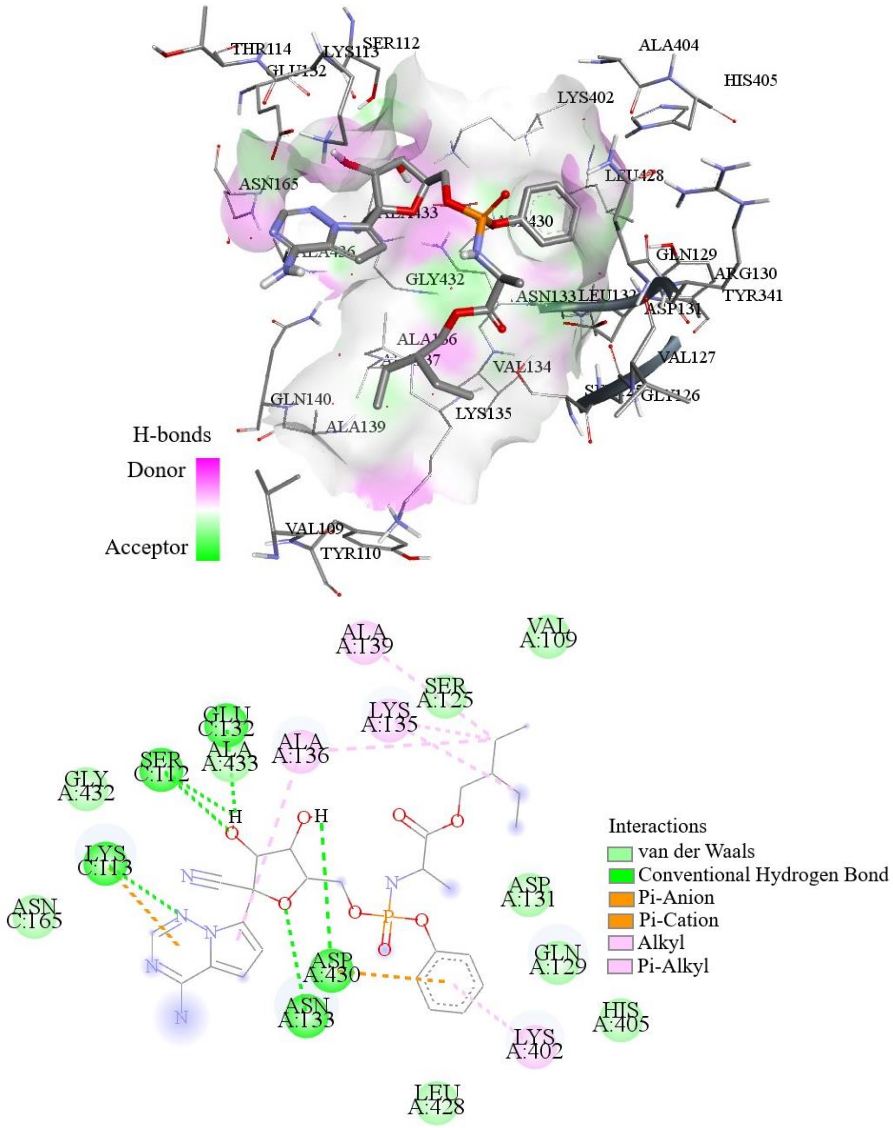

Fig. 5. The interacting residues of corresponding chains of the S protein and furin protease (gray) with remdesivir (coloring by element, all C atoms of ligand are in dark gray, red — O, gray — H, blue — N) are labeled and shown as stick models. The ligand interaction diagram of remdesivir with the 6VYB-5JXG complex is shown, and the types of intermolecular interactions are labeled.

However, hydrogen bonds are formed with the S protein's C chain (Lys113, Ser112, and Glu132) and the furin protease (Asn133, Asp430, and Ala433). In the complex 6VXX-5JXG, remdesivir forms hydrogen bonds (Thr29, His194, Asp215, and Thr365) and hydrophobic interaction (Asp191, and His364) only with furin (Fig. 6).

Our docking studies showed that remdesivir directly targets the furin cleavage site of the S protein (in the 7VHJ-5JXG complex), forming an energetically favorable complex through hydrogen bonds and hydrophobic interactions with high binding affinity. Remdesivir interacts with 7VHJ-5JXG with the high binding energy score of -9.1 kcal/mol. The molecular binding is stabilized through hydrogen bonds with Asp174, Asp179, and Gln183 of furin, as well as Ser679,

and Ala681 of the S protein. Hydrophobic interactions are mediated by Arg357 of furin and Ser682 of the S protein, while π-stacking interactions involve Tyr186 of furin (Fig. 7).

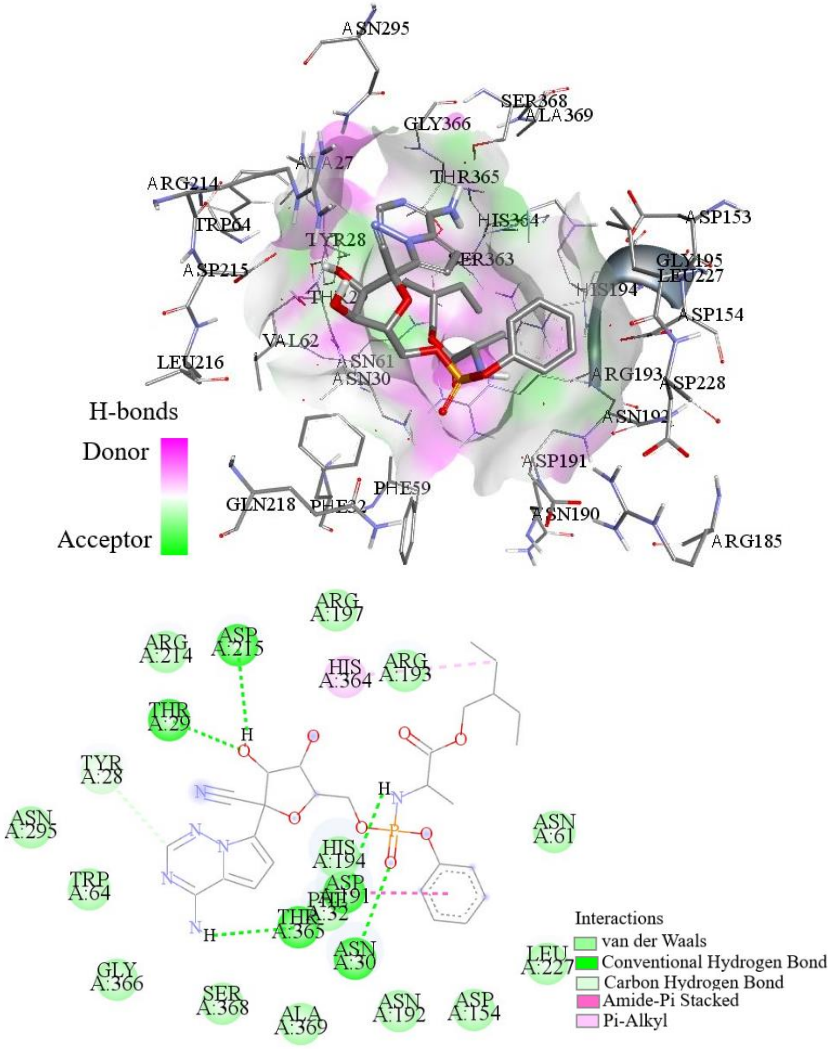

Fig. 6. The interacting residues of furin protease (gray) with remdesivir (coloring by element, all C atoms of ligand are in dark gray, red — O, gray — H, blue — N) are labeled and shown as stick models. The ligand interaction diagram of remdesivir with the 6VXX-5JXG complex is shown, and the types of intermolecular interactions are labeled.

Remdesivir, which has moderate lipophilicity (logP = 1.9), showed corresponding binding affinity to the complexes – particularly to complex 7VGH-5JXG – through interactions with Ser682, Ala681, and Ser679 (Fig. 7). In general, remdesivir exhibits specificity for RNA-dependent RNA polymerase. Upon conversion to its active hydrophilic metabolite (GS-441524) within the cell, remdesivir mimics a nucleoside and incorporates into viral RNA during replication [39].

Our binding affinity calculations using AutoDock Vina for nelfinavir showed that the binding affinities with the S protein-furin protease complexes ranged from -8.2 kcal/mol to -9.3 kcal/mol. We showed that the SARS-CoV-2 S protein-furin complex (7VHJ-5JXG), which includes amino acid residues of the furin cleavage site, interacts with nelfinavir with the highest binding affinity of -9.3 kcal/mol (Fig.8). At the same time, the binding affinities decreased with

a reduction in the total number of contacts (hydrogen bonds and hydrophobic interactions) between nelfinavir and furin protease of this complex.

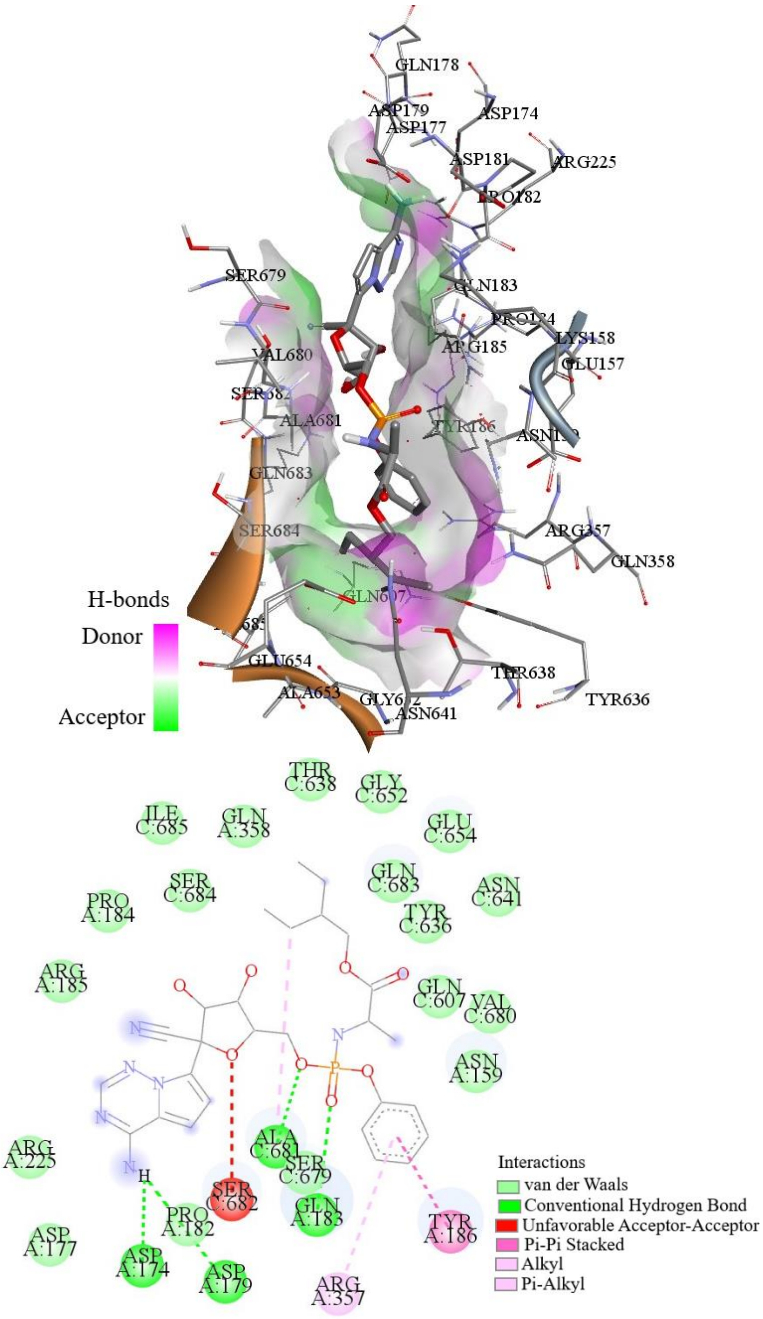

Fig. 7. The interacting residues of corresponding chains of the S protein (brown) and furin protease (gray) with remdesivir (coloring by element, all C atoms of ligand are in dark gray, red — O, gray — H, blue — N) are labeled and shown as stick models. The ligand interaction diagram of remdesivir with the 7VHJ-5JXG complex is shown, and the types of intermolecular interactions are labeled.

Furthermore, our protein-ligand docking results align with those of Bashir and co-authors, who identified Ser368, Thr365, and His364 as key residues in the binding active site of furin [31]. Our findings demonstrated that the high affinity of nelfinavir for 7VHJ-5JXG is primarily due to the formation of hydrogen bonds with His364, and Thr365 of the furin protease.

Additionally, hydrophobic interactions involving His194, and Leu227 of furin and Arg214 of the S protein contributed to the conformational stability of the 7VHJ-5JXG-nelfinavir complex. Trp64 of the S protein forms an electrostatic interaction with the ligand.

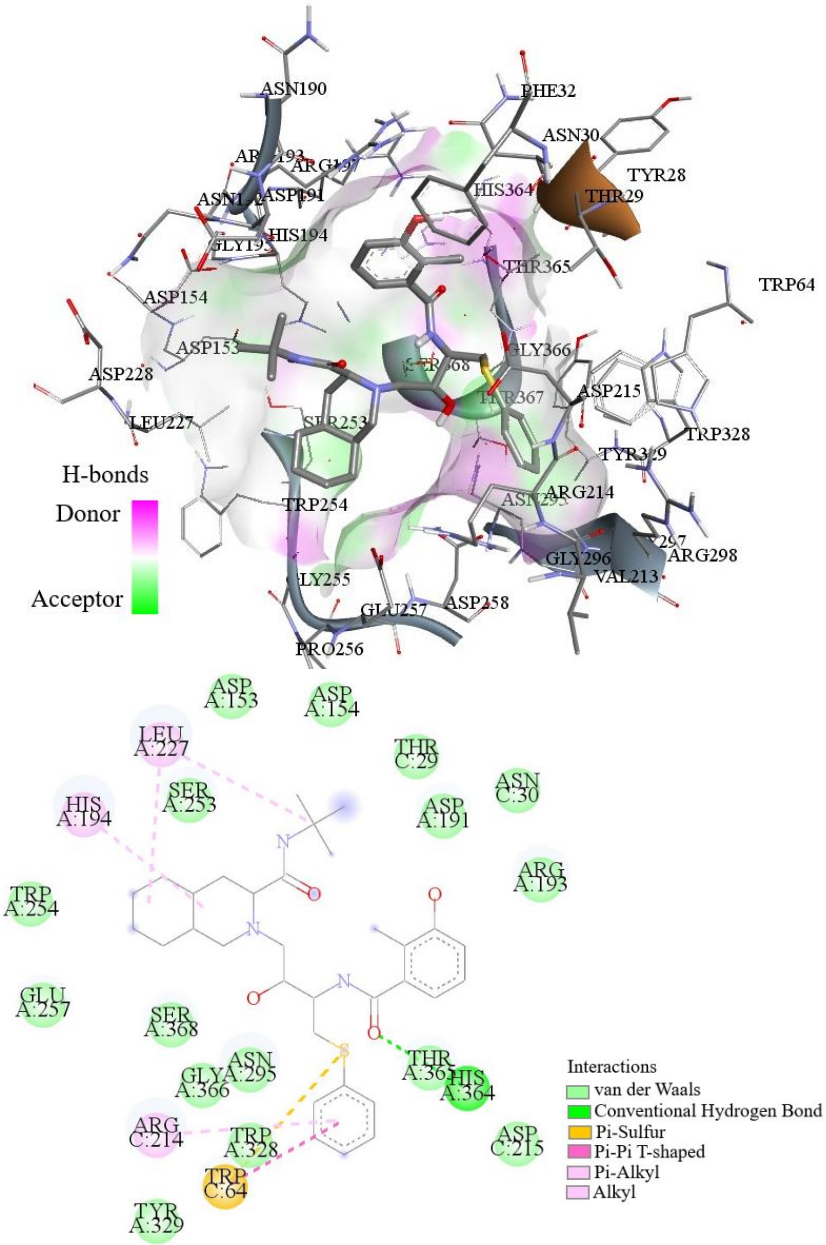

Fig.8. The key intermolecular interactions between nelfinavir and the 7VHJ-5JXG complex are shown. The interacting residues of corresponding chains of the S protein (brown) and furin protease (gray) with nelfinavir (coloring by element, all C atoms of ligand are in dark gray, red — O, gray — H, blue — N) are labeled and shown as stick models. 2D ligand interaction diagrams between nelfinavir and the 7VHJ-5JXG complex are shown. Various types of intermolecular interactions are labeled in the legend.

The catalytic domain of furin has a cavity with an active site surrounded by negatively charged residues. This configuration allows inhibitors to bind to the enzyme and interact with the catalytic triad — Asp153, His194, and Ser368 — essential for its catalytic activity by hydrolyzing the virus' peptide bonds [40]. Our studies showed that nelfinavir and PI8 bind favorably to the catalytic domain of furin, especially of the 7VHJ-5JXG complex.

We demonstrated that the lipophilicity of nelfinavir influences the binding affinity of the studied complexes. Nelfinavir contains benzene rings and aliphatic chains, which enable it to specifically interact with the hydrophobic pockets of these complexes. These pockets are formed by hydrophobic amino acid residues, particularly in complex 7VGH-5JXG, where Trp64 and Leu227 play a key role (Fig. 8).

Chloroquine is known to have a broad spectrum of antiviral activity and is primarily used for the prevention and treatment of malaria and rheumatic diseases [41]. However, it has been found to interact with ACE2 and the coronavirus spike protein by inhibiting ACE2, thereby suppressing the replication of SARS-CoV-2.

We have shown that chloroquine binds to amino acid residues of the receptor-binding domain (RBD) of the spike protein in its "closed" conformation through interactions with Phe515 (via hydrogen bonding); Phe464, Pro426, and Leu518 (via hydrophobic interactions); and Glu516 (via electrostatic π-anion interaction). The binding energy score was -6.3 kcal/mol, which is consistent with the findings reported in Badrauli's work [42].

As noted by Khatabi, chloroquine can also bind to nonstructural proteins. The binding affinity of chloroquine to the SARS-CoV-2 main protease was -3.07 kcal/mol, which is lower than its affinity for ACE2. The stability of the SARS-CoV-2 main protease–chloroquine complex was provided by the same nonpolar hydrophobic amino acid residues as in our study, such as phenylalanine, valine, proline, and leucine [43]. The presence of benzene rings contributes to chloroquine's high lipophilicity (logP = 4.6) and facilitates its hydrophobic interactions with nonpolar amino acid residues in chain C of the S protein, including Val126, Ile119, Phe194, Trp104, and Ile203 (figure not shown).

In the 6VYB-5JXG and 6XXV-5JXG structures, favipiravir demonstrated the lowest binding affinity of -5.9 kcal/mol and -5.8 kcal/mol, respectively, which are consistent with the results of Eweas A.F. et al. [38].

It is known that favipiravir is a target-specific drug that acts as a substrate for the RNA-dependent RNA polymerase, thereby preventing viral transcription and replication [44]. Favipiravir has also been reported as an antiviral option against the main viral protease of SARS-CoV-2, although it was originally developed to treat influenza. Molecular docking results showed a strong binding affinity (-4.4 kcal/mol) and numerous interactions, including both hydrogen bonds and hydrophobic contacts [45].

Our study demonstrated that, unlike other studied ligands, favipiravir forms an energetically favorable complex with the B chain of the S protein in the "open" conformation of 6VYB-5JXG through a hydrogen bond (with Asn354), a hydrophobic interaction (with Ala344), and a halogen bond (with Val341). In the 6XXV-5JXG and 7VHJ-5JXG structures, favipiravir binds only to furin amino acid residues through hydrogen bonds (Glu157, Pro256, Asp306, Ala292), hydrophobic interaction (Tyr186), and halogen bonds (Glu654, Gln183, Asp301, Glu331) (figures not shown). Favipiravir contains polar functional groups that result in low lipophilicity (logP = -0.6), and thus it tends to interact with hydrophilic or polar amino acids such as tyrosine and glutamic acid.

Summarizing the docking results of five ligands investigated as potential inhibitors of the S protein–furin complex, it is notable that PI8 and remdesivir form interactions with all three complexes analyzed. These contacts occur directly within the active site of furin. Nelfinavir and favipiravir also interact with the furin active site, although only in two of the three investigated complexes. In contrast, chloroquine does not interact with the furin active site; instead, it binds solely to the C chain of the S protein, i.e., outside the furin cleavage site. To date, despite numerous studies on the therapeutic potential of chloroquine for the treatment of COVID-19 and its demonstrated antiviral and anti-inflammatory properties, the precise mechanism of its action remains insufficiently understood. In particular, it is still unclear

whether there are specific molecular targets in the SARS-CoV-2 life cycle that can be inhibited by chloroquine [25].

These concluding remarks support the promising antiviral properties of PI8, remdesivir, nelfinavir, and favipiravir against a broad range of RNA viruses [35–38, 45], including their potential as inhibitors of SARS-CoV-2 protein complexes at the molecular level. At the same time, the unexplored potential of chloroquine as a possible inhibitor of certain viral molecular targets warrants further investigation.

CONCLUSIONS

Our results demonstrate that furin can interact with the S protein in both "open" and "closed" conformations, even outside the canonical furin cleavage site. These interactions indicate alternative mechanisms for the S protein–furin binding, potentially compensating for the unmodeled structure of the region containing the furin cleavage site. Moreover, the fully modeled structure of the furin cleavage site in the 7VHJ structure facilitated an energetically favorable, near-canonical interaction involving the fusion peptide and the heptapeptide repeat sequence 1.

This study also showed that, regardless of furin's binding location on the S protein, inhibitors preferentially bind to furin — particularly at its catalytic site — rather than to the S protein within the investigated SARS-CoV-2 S protein–furin complexes, thereby preventing S protein processing. The potential binding sites of several non-specific antiviral drugs, including remdesivir, chloroquine, favipiravir, nelfinavir, and PI8, were evaluated on the 6VYB-5JXG, 6VXX-5JXG, and 7VHJ-5JXG structures.

In silico docking study was performed using the target docking mode of AutoDock Vina. Screening of all ligands revealed that PI8, nelfinavir, and remdesivir exhibited the highest binding affinity for the 7VHJ-5JXG structure, likely due to the fully modeled structure of the furin cleavage site. The binding energy scores were -9.9 kcal/mol for PI8, -9.3 kcal/mol for nelfinavir, and -9.1 kcal/mol for remdesivir.

A detailed atomic-level understanding of S protein–furin interactions with antiviral agents, enabled by molecular docking technologies, could support the development of new therapeutic agents or drug combinations to combat COVID-19. Therefore, this study of inhibitors targeting the SARS-CoV-2 S protein–furin protease complex provides valuable insights for assessing these compounds as potential antiviral drugs against SARS-CoV-2.

CONFLICT OF INTEREST

The authors report that there is no conflict of interest.

Authors' ORCID ID

N. V. Khmil https://orcid.org/0000-0001-7916-5921
A. V. Shestopalova https://orcid.org/0000-0001-7613-7212

REFERENCES

1. WHO. 2020. Coronavirus disease 2019 (COVID-19) weekly epidemiological updates. Available from: https://www.who.int/emergencies/diseases/novel-coronavirus-2019/situation-reports
2. Sanche S, Lin YT, Xu C, Romero-Severson E, Hengartner N, Ke R. High contagiousness and rapid spread of severe acute respiratory syndrome coronavirus 2. Emerg Infect Dis. 2020;26(7):1470–77. https://doi.org/10.3201/eid2607.200282
3. Sanders JM, Monogue ML, Jodlowski TZ, Cutrell JB. Pharmacologic treatments for coronavirus disease 2019 (COVID-19): A Review. JAMA. 2020;323(18):1824–36. https://doi.org/10.1001/jama.2020.6019
4. Khmil NV, Kolesnikov VG, Boiechko-Nemovcha AO. Binding characteristics of systemic glucocorticoids to the SARS-CoV-2 spike glycoprotein: in silico evaluation. Low Temp Phys. 2025;51:96–103 https://doi.org/10.1063/10.0034652

5. Zhang L, Lin D, Sun X, Curth U, Drosten C, Sauerhering L, et al. Crystal structure of SARS-CoV-2 main protease provides a basis for design of improved α-ketoamide inhibitors. Science. 2020;368(6489):409-12. https://doi.org/10.1126/science.abb3405
6. Khmil NV, Shestopalova AV, Kolesnikov VG, Boiechko-Nemovcha AO. Identification of potential corticosteroid binding sites on the SARS CoV-2 main protease Mpro- in silico docking study. Biophysical Bulletin. 2024;51:53–63. https://doi.org/10.26565/2075-3810-2024-51-04
7. Huang Y, Yang C, Xu XF, Xu W, Liu SW. Structural and functional properties of SARS-CoV-2 spike protein: potential antivirus drug development for COVID-19. Acta Pharmacol Sin. 2020;41(9):1141–49. https://doi.org/10.1038/s41401-020-0485-4
8. Zhang J, Xiao T, Cai Y, Chen B. Structure of SARS-CoV-2 spike protein. Curr Opin Virol. 2021;50:173–82. https://doi.org/10.1016/j.coviro.2021.08.010
9. Hulswit RJ, de Haan CA, Bosch BJ. Coronavirus spike protein and tropism changes. Adv Virus Res. 2016;96:29–57. https://doi.org/10.1016/bs.aivir.2016.08.004
10. Cai Y, Zhang J, Xiao T, Peng H, Sterling SM, Walsh RM, et al. Distinct conformational states of SARS-CoV-2 spike protein. Science. 2020;369(6511):1586–92. https://doi.org/10.1126/science.abd4251
11. Gur M, Taka E, Yilmaz SZ, Kilinc C, Aktas U, Golcuk M. Conformational transition of SARS-CoV-2 spike glycoprotein between its closed and open states. J Chem Phys. 2020;153(7):075101. https://doi.org/10.1063/5.0011141
12. Hoffmann M, Kleine-Weber H, Pöhlmann S. A Multibasic cleavage site in the spike protein of SARS-CoV-2 is essential for Infection of human lung cells. Mol Cell. 2020;78(4):779-84.e5. https://doi.org/10.1016/j.molcel.2020.04.022
13. Strobelt R, Adler J, Shaul Y. The Transmembrane protease serine 2 (TMPRSS2) non-protease domains regulating severe acute respiratory syndrome coronavirus 2 (SARS-CoV-2) spike-mediated virus entry. Viruses. 2023;15(10):2124. https://doi.org/10.3390/v15102124
14. Marcink TC, Kicmal T, Armbruster E, Zhang Z, Zipursky G, Golub KL, et al. Intermediates in SARS-CoV-2 spike-mediated cell entry. Sci Adv. 2022;8(33):eabo3153. https://doi.org/10.1126/sciadv.abo3153
15. Peacock TP, Goldhill DH, Zhou J, Baillon L, Frise R, Swann OC, et al. The furin cleavage site in the SARS-CoV-2 spike protein is required for transmission in ferrets. Nat Microbiol. 2021;6(7):899–909. https://doi.org/10.1038/s41564-021-00908-w
16. Coutard B, Valle C, de Lamballerie X, Canard B, Seidah NG, Decroly E. The spike glycoprotein of the new coronavirus 2019-nCoV contains a furin-like cleavage site absent in CoV of the same clade. Antiviral Res. 2020;176:104742. https://doi.org/10.1016/j.antiviral.2020.104742
17. Holmes EC, Goldstein SA, Rasmussen AL, Robertson DL, Crits-Christoph A, Wertheim JO, et al. The origins of SARS-CoV-2: A critical review. Cell. 2021;184(19):4848–56. https://doi.org/10.1016/j.cell.2021.08.017
18. Cheng YW, Chao TL, Li CL, Chiu MF, Kao HC, Wang SH, et al. Furin inhibitors block SARS-CoV-2 spike protein cleavage to suppress virus production and cytopathic effects. Cell Rep. 2020;33(2):108254. https://doi.org/10.1016/j.celrep.2020.108254
19. Brown AJ, Won JJ, Graham RL, Dinnon KH, Sims AC, Feng JY, et al. Broad spectrum antiviral remdesivir inhibits human endemic and zoonotic deltacoronaviruses with a highly divergent RNA dependent RNA polymerase. Antiviral Res. 2019;169:104541. https://doi.org/10.1016/j.antiviral.2019.104541
20. Nguyen TH, Guedj J, Anglaret X, Laouénan C, Madelain V, Taburet AM, et al. Favipiravir pharmacokinetics in Ebola-Infected patients of the JIKI trial reveals concentrations lower than targeted. PLoS Negl Trop Dis. 2017;11(2):e0005389. https://doi.org/10.1371/journal.pntd.0005389
21. Garriga C, Pérez-Elías MJ, Delgado R, Ruiz L, Nájera R, Pumarola T, et al. Mutational patterns and correlated amino acid substitutions in the HIV-1 protease after virological failure to nelfinavir- and lopinavir/ritonavir-based treatments. J Med Virol. 2007;79(11):1617–28. https://doi.org/10.1002/jmv.20986
22. Agostini ML, Andres EL, Sims AC, Graham RL, Sheahan TP, Lu X, et al. Coronavirus susceptibility to the antiviral remdesivir (GS-5734) is mediated by the viral polymerase and the proofreading exoribonuclease. mBio. 2018;9(2):e00221-18. https://doi.org/10.1128/mBio.00221-18
23. Grein J, Ohmagari N, Shin D, Diaz G, Asperges E, Castagna A, et al. Compassionate use of remdesivir for patients with severe Covid-19. N Engl J Med. 2020;382(24):2327–36. https://doi.org/10.1056/NEJMoa2007016
24. Driouich JS, Cochin M, Lingas G, Moureau G, Touret F, Petit PR, et al. Favipiravir antiviral efficacy against SARS-CoV-2 in a hamster model. Nat Commun. 2021;12(1):1735. https://doi.org/10.1038/s41467-021-21992-w

25. Jia Y, Tian W, Li Y, Teng Y, Liu X, Li Z, et al. Chloroquine: Rapidly withdrawing from first-line treatment of COVID-19. Heliyon. 2024;10(17):e37098. https://doi.org/10.1016/j.heliyon.2024.e37098
26. Søndergaard CR, Olsson MH, Rostkowski M, Jensen JH. Improved treatment of ligands and coupling effects in empirical calculation and rationalization of pKa values. J Chem Theory Comput. 2011;7(7):2284–95. https://doi.org/10.1021/ct200133y
27. Trott O, Olson AJ. AutoDock Vina: improving the speed and accuracy of docking with a new scoring function, efficient optimization, and multithreading. J Comput Chem. 2010;31(2):455–61. http://doi.org/10.1002/jcc.21334
28. O'Boyle NM, Banck M, James CA, Morley C, Vandermeersch T, Hutchison GR. Open Babel: An open chemical toolbox. J Cheminform. 2011;3:33. https://doi.org/10.1186/1758-2946-3-33
29. Dahms SO, Jiao GS, Than ME. Structural studies revealed active site distortions of human furin by a small molecule inhibitor. ACS Chem Biol. 2017;12(5):1211–16. https://doi.org/10.1021/acschembio.6b01110
30. Kozakov D, Brenke R, Comeau SR, Vajda S. PIPER: an FFT-based protein docking program with pairwise potentials. Proteins. 2006;65(2):392–406. https://doi.org/10.1002/prot.21117
31. Bashir A, Li S, Ye Y, Zheng Q, Knanghat R, Bashir F, et al. SARS-CoV-2 S protein harbors furin cleavage site located in a short loop between antiparallel β-strand. Int J Biol Macromol. 2024;281(Pt 1):136020. https://doi.org/10.1016/j.ijbiomac.2024.136020
32. Vankadari N. Structure of furin protease binding to SARS-CoV-2 spike glycoprotein and implications for potential targets and virulence. J Phys Chem Lett. 2020;11(16):6655–63. https://doi.org/10.1021/acs.jpclett.0c01698
33. Bollavaram K, Leeman TH, Lee MW, Kulkarni A, Upshaw SG, Yang J, et al. Multiple sites on SARS-CoV-2 spike protein are susceptible to proteolysis by cathepsins B, K, L, S, and V. Protein Sci. 2021;30(6):1131–43. https://doi.org/10.1002/pro.4073
34. Bosch BJ, Bartelink W, Rottier PJ. Cathepsin L functionally cleaves the severe acute respiratory syndrome coronavirus class I fusion protein upstream of rather than adjacent to the fusion peptide. J Virol. 2008;82(17):8887–90. https://doi.org/10.1128/JVI.00415-08
35. Van Lam van T, Ivanova T, Hardes K, Heindl MR, Morty RE, Böttcher-Friebertshäuser E, et al. Design, synthesis, and characterization of macrocyclic inhibitors of the proprotein convertase furin. ChemMedChem. 2019;14(6):673–85. https://doi.org/10.1002/cmdc.201800807
36. Gordon CJ, Tchesnokov EP, Woolner E, Perry JK, Feng JY, Porter DP, et al. Remdesivir is a direct-acting antiviral that inhibits RNA-dependent RNA polymerase from severe acute respiratory syndrome coronavirus 2 with high potency. J Biol Chem. 2020;295(20):6785–97. https://doi.org/10.1074/jbc.RA120.013679
37. Nguyen HL, Thai NQ, Truong DT, Li MS. Remdesivir strongly binds to both RNA-dependent RNA polymerase and main protease of SARS-CoV-2: evidence from molecular simulations. J Phys Chem B. 2020;124(50):11337–48. https://doi.org/10.1021/acs.jpcb.0c07312
38. Eweas AF, Alhossary AA, Abdel-Moneim AS. Molecular docking reveals ivermectin and remdesivir as potential repurposed drugs against SARS-CoV-2. Front Microbiol. 2021;11:592908. https://doi.org/10.3389/fmicb.2020.592908
39. Sukeishi A, Itohara K, Yonezawa A, Sato Y, Matsumura K, Katada Y, et al. Population pharmacokinetic modeling of GS-441524, the active metabolite of remdesivir, in Japanese COVID-19 patients with renal dysfunction. CPT: Pharmacomet Syst Pharmacol. 2022;11(1):94–103. https://doi.org/10.1002/psp4.12736
40. Thomas G. Furin at the cutting edge: from protein traffic to embryogenesis and disease. Mol Cell biol. 2002;3(10):753–66. https://doi.org/10.1038/nrm934
41. Jorge A, Ung C, Young LH, Melles RB, Choi HK. Hydroxychloroquine retinopathy - implications of research advances for rheumatology care. Nat Rev Rheumatol. 2018;14(12):693–703. https://doi.org/10.1038/s41584-018-0111-8
42. Badraoui R, Adnan M, Bardakci F, Alreshidi MM. Chloroquine and hydroxychloroquine interact differently with ACE2 domains reported to bind with the coronavirus spike protein: mediation by ACE2 polymorphism. Molecules. 2021;26(3):673. https://doi.org/10.3390/molecules26030673
43. El Khatabi K, Aanouz I, Alaqarbeh M, Ajana MA, Lakhlifi T, Bouachrine M. Molecular docking, molecular dynamics simulation, and ADMET analysis of levamisole derivatives against the SARS-CoV-2 main protease (M^{Pro}). Bioimpacts. 2022;12(2):107–13. https://doi.org/10.34172/bi.2021.22143
44. Shannon A, Selisko B, Le NT, Huchting J, Touret F, Piorkowski G, et al. Rapid incorporation of favipiravir by the fast and permissive viral RNA polymerase complex results in SARS-CoV-2 lethal mutagenesis. Nat Commun. 2020;11(1):4682. https://doi.org/10.1038/s41467-020-18463-z

45. Yadav P, Rana M, Chowdhury P. DFT and MD simulation investigation of favipiravir as an emerging antiviral option against viral protease (3CL^{pro}) of SARS-CoV-2. J Mol Struct. 2021;1246:131253. https://doi.org/10.1016/j.molstruc.2021.131253

АНАЛІЗ IN SILICO САЙТІВ ЗВ'ЯЗУВАННЯ ПОТЕНЦІЙНИХ ІНГІБІТОРІВ КОМПЛЕКСУ ФУРИНОВОЇ ПРОТЕАЗИ ТА СПАЙК БІЛКА SARS-COV-2

Н. В. Хміль[1,2], А. В. Шестопалова[2], В. Г. Колесніков[2]

[1]Харківський національний університет радіоелектроніки, пр. Науки, 14, Харків, 61166, Україна;
[2]Інститут радіофізики та електроніки ім. О. Я. Усикова НАН України, вул. Ак. Проскури, 12, Харків, 61085, Україна
e-mail: khmilnatali@gmail.com

Надійшла до редакції 28 квітня 2025 р. Переглянута 7 липня 2025 р.
Прийнята до друку 29 серпня 2025 р.

Актуальність. COVID-19 — це інфекційне захворювання, спричинене коронавірусом важкого гострого респіраторного синдрому (SARS-CoV-2). Зусилля у боротьбі з вірусом включають розробку та дослідження вакцин, моноклональних антитіл і специфічних противірусних препаратів, спрямованих на важливі мішені у життєвому циклі вірусу.
Мета роботи. Метою цього дослідження є вивчення потенційних сайтів зв'язування фуринової протеази з S-білком у різних конформаціях та оцінка спорідненості зв'язування неспецифічних противірусних препаратів та макроциклічного пептидоміметичного інгібітора 8 (PI8) з комплексом S-білок-фуринова протеаза методом молекулярного докінгу.
Матеріали та методи. Тривимірні структури S білка (PDB IDs: 6VYB, 6VXX, 7VHJ) з бази даних PDB (www.rcsb.org) були стиковані до фуринової протеази (PDB ID: 5JXG) за допомогою сервера ClusPro 2.0. Неспецифічні противірусні препарати, такі як ремдесивір, хлорохін, фавіпіравір, нелфінавір, а також PI8, були стиковані до комплексів 6VYB-5JXG, 6VXX-5JXG і 7VHJ-5JXG за допомогою AutoDock Vina. Ліганди були енергетично мінімізовані за допомогою універсального силового поля (UFF) і конвертовані у формат PDBQT за допомогою OpenBabel. Оптимізація білків здійснювалася з використанням інструментів AutoDock. Результати докінгу були візуалізовані у програмі Discovery Studio 2024.
Результати. Спорідненість зв'язування досліджених лігандів із комплексами S-білок–фуринова протеаза підтверджена результатами молекулярного докінгу. PI8, нелфінавір і ремдесивір показали високу спорідненість зв'язування зі структурою 7VHJ-5JXG через визначеність структури у сайті розщеплення фурином. Найкращі результати молекулярного докінгу для PI8 з комплексами 6VYB-5JXG, 6VXX-5JXG і 7VHJ-5JXG становлять -9.7 ккал/моль, -9.5 ккал/моль і -9.9 ккал/моль відповідно. Взаємодія між комплексами S-білок–фуринова протеаза і PI8 відбувається через специфічні амінокислотні залишки, розташовані головним чином у каталітичному центрі фурину та петлі реактивного сайту PI8. Дослідження показали, що ремдесивір безпосередньо впливає на сайт розщеплення фурином S білка (у комплексі 7VHJ-5JXG), утворюючи енергетично сприятливі взаємодії завдяки водневим зв'язкам і гідрофобним контактам із високою спорідненістю зв'язування (енергетичний показник зв'язування становив -9.1 ккал/моль). Енергетично сприятливі взаємодії комплексів 6VYB-5JXG, 6VXX-5JXG і 7VHJ-5JXG з нелфінавіром також підтверджуються низькими енергетичними показниками, які становлять -8.2 ккал/моль, -8.9 ккал/моль і -9.3 ккал/моль відповідно.
Висновки. Згідно з результатами молекулярного докінгу, PI8, нелфінавір і ремдесивір демонструють енергетично сприятливі взаємодії з досліджуваними комплексами та мають потенціал для використання як перспективні інгібітори, спрямовані на комплекси SARS-CoV-2 S-білка з фуриновою протеазою.
КЛЮЧОВІ СЛОВА: спайк білок SARS-CoV-2; фуринова протеаза; противірусні препарати; молекулярний докінг; здоров'я людини.